

First Demonstration of Subsystem-Modular Optical Cross-Connect Using Single-Module 6×6 Wavelength-Selective Switch

Ryota Hashimoto^{ID}, Shuhei Yamaoka, Yojiro Mori, *Member, IEEE*, Hiroshi Hasegawa, *Member, IEEE*, Ken-Ichi Sato^{ID}, *Fellow, IEEE*, Keita Yamaguchi, *Member, IEEE*, Kazunori Seno, *Member, IEEE*, and Kenya Suzuki^{ID}, *Member, IEEE*

(Highly-Scored Paper)

Abstract—We demonstrate a highly scalable subsystem-modular optical cross-connect (OXC) that uses sub-OXCs based on a newly developed single-module 6×6 wavelength-selective switch (WSS). Network simulations in dynamic-traffic scenarios assure the good routing performance of the architecture. Its technical feasibility is confirmed by transmission experiments using 96-wavelength 32-Gbaud dual-polarization quadrature phase-shift keying (DP-QPSK) signals. The developed 6×6 WSS allows each DP-QPSK signal to traverse 12 nodes when the internode distance is 100 km.

Index Terms—Optical cross-connect, photonic network, wavelength-selective switch.

I. INTRODUCTION

THE optical cross-connect (OXC) can route optical signals without costly optical-electrical-optical (OEO) conversion and hence enhance fiber-utilization efficiency of the network cost-effectively. To maximize the utilization efficiency of link fibers, OXCs should possess non-restricted routing capability other than the inherent restriction of wavelength collision in a fiber. The currently deployed non-restricted small-scale OXC utilizes multiple $1 \times L$ wavelength-selective switches (WSSs) to attain fully flexible routing. Since the network traffic is rapidly increasing especially in metro areas [1], the OXC must accommodate a large number of input/output ports while satisfying the unique requirements for metro networks. Table I compares OXC requirements in metro networks with those in core networks [2]. Network cost consists of link cost and node cost

TABLE I
COMPARISON OF OXCS FOR METRO AND CORE NETWORKS

	Core network	Metro network
Transmission distance	Longer	Shorter
Acceptable node cost	Larger	Smaller
OXC port count	Small	Small to large (Large variation)

(operation cost is another important factor, but it is not discussed herein). The OXC can maximize fiber utilization with its optical path add/drop capability; its wavelength routing capability eliminates most of the expensive OEO conversions that would otherwise be needed. Therefore, there is no benefit to introducing costly OXCs if the relative link cost is very small. The transmission distance in metro networks is shorter than that in core networks, and hence the acceptable OXC cost in the metro network must be smaller than that in the core network. The metro traffic is increasing rapidly and so the required OXC port-count is likely to become large in the future; however, the OXC should be introduced cost-effectively from the outset, in other words pay-as-you-grow capability is necessary. Further, the traffic distribution in a metro network can be very non-uniform, data centers or video center can be localized and, as a result, the nodes will require different OXC port-counts. The key attributes of the OXC for metro networks are its cost-effectiveness and ease of expansion.

The current OXC structure cannot match these attributes. The present OXC generally adopts the broadcast-and-select architecture (splitters-&-WSSs) [3]. As the OXC port count increases, the splitter loss and crosstalk at the WSSs become excessive. To avoid this, the route-and-select architecture (WSSs-&-WSSs) must be employed [3]. In the future, we may need to concatenate multiple WSSs to create a high-port-count WSS since the port count of current WSSs is limited to around 30. With the concatenation, the number of $1 \times L$ WSSs needed in creating an $N \times N$ OXC is given by $\text{ceil}(N/L) \times N \times C$, where $C = 1$ for the broadcast-and-select architecture and $C = 2$ for the route-and-select one (here the first stage is assumed to use an optical coupler, but if we use a WSS, more WSSs are needed). Thus, the number of costly WSSs increases super-linearly against the

Manuscript received October 23, 2017; revised January 19, 2018; accepted January 26, 2018. Date of publication January 30, 2018; date of current version March 1, 2018. This work was supported in part by NICT and KAKENHI (26220905). (Corresponding author: Ryota Hashimoto.)

R. Hashimoto, S. Yamaoka, Y. Mori, H. Hasegawa, and K.-I. Sato are with the Department of Information and Communication Engineering, Nagoya University, Nagoya 464-8603, Japan (e-mail: r_hashimo@echo.nuee.nagoya-u.ac.jp; yamaoka.shuhei@j.mbox.nagoya-u.ac.jp; mori@nuee.nagoya-u.ac.jp; hasegawa@nuee.nagoya-u.ac.jp; sato@nuee.nagoya-u.ac.jp).

K. Yamaguchi and K. Seno are with the NTT Device Technology Laboratories, Kanagawa 243-0198, Japan (e-mail: yamaguchi.keita@lab.ntt.co.jp; seno.kazunori@lab.ntt.co.jp).

K. Suzuki is with the NTT Network Innovation Laboratories, Tokyo 180-0012, Japan (e-mail: s.kenya@lab.ntt.co.jp).

Color versions of one or more of the figures in this paper are available online at <http://ieeexplore.ieee.org>.

Digital Object Identifier 10.1109/JLT.2018.2800082

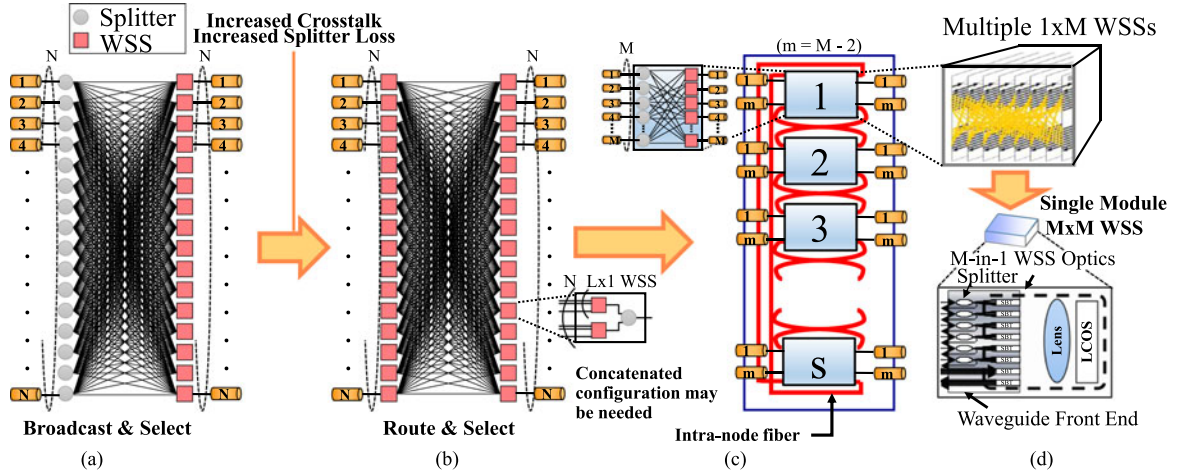


Fig. 1. OXC configurations: conventional large-scale OXC using (a) broadcast-and-select approach and (b) route-and-select approach, (c) subsystem-modular OXC with $1 \times M$ WSSs, and (d) $M \times M$ WSSs used as sub-OXCs.

needed OXC port count. Furthermore, OXC port-count expansion is not easy. Given the future traffic growth expected, the large port count OXC or the component, large port count WSSs, needs to be implemented at the day one. Port count expansion is possible up to the designed maximum number; however, installing a pair of WSSs (input and output sides) causes new fiber interconnections. The designed maximum port count greatly constricts expansion capability and human labor is needed.

To resolve the problems while satisfying the requirements for future metro networks, we investigate the suitability of the subsystem-modular OXC using $M \times M$ WSS [4], [5] to metro networks. Here, ‘ $M \times M$ ’ means that optical paths accommodated in the M input ports can be connected to M output ports with no restriction other than the inherent restriction of wavelength collision in a fiber. This OXC architecture parallelizes multiple small-scale OXC subsystems (sub-OXCs) via a limited number of intra-node fibers that connect distinct $M \times M$ WSSs. Since the OXC port count can be expanded by simply adding sub-OXCs, cost-effective deployment of diverse-port-count OXCs can be realized. The subsystem-modular OXC is most simply implemented by using $M \times M$ WSSs [5], and intensive development efforts are under way [6]–[11]. Recently, a new type of $M \times M$ WSS has been developed that uses a spatial and planar optical circuit (SPOC) [7], [11].




In this paper, we demonstrate a subsystem-modular OXC that utilizes a 6×6 WSS prototype as a sub-OXC. The 6×6 WSS prototype was fabricated using SPOC technology. First, we analyze the applicability of 6×6 WSSs to metro networks from the networking viewpoint via computer simulations under dynamic traffic scenarios. The simulation results prove that our OXC architecture offers virtually the same routing performance as the equivalent-scale single OXC with no routing restrictions. Second, we construct part of a large-scale OXC by using the developed 6×6 WSS. The transmission performance of the OXC is experimentally evaluated using 96-wavelength 32-Gbaud dual-polarization quadrature phase-shift keying (DP-QPSK) signals on the 50-GHz grid. The signals can traverse 12 nodes when the inter-node distance is 100 km. To the best of our knowledge, this is the first experimental demonstration of a large-

scale OXC based on $M \times M$ WSSs. A preliminary version of this paper was presented at the European Conference on Optical Communication [12].

II. SUBSYSTEM-MODULAR OXC ARCHITECTURE

To process a large amount of network traffic expected in the future, the OXC must offer a large number of input/output ports. Fig. 1(a) shows a large-scale non-restricted OXC employing the broadcast-and-select architecture. Signals can be routed without any restriction since all input ports are connected to all output ports. However, this OXC architecture cannot accommodate large port counts since the splitter loss and cross talk at the WSS become excessive. To avoid the large splitter loss, the route-and-select architecture [see Fig. 1(b)] must be employed, which doubles the number of necessary WSSs. Furthermore, since the maximum total port count of practical WSSs is limited, multiple WSSs may be used in parallel [cf. insert in Fig. 1(b)], which further increases the number of necessary WSSs and triggers more complicated fiber connection inside the OXC. The subsystem-modular OXC architecture [see Fig. 1(c)] consists of small-scale sub-OXCs, and hence using the cost-effective broadcast-and-select architecture is possible; the number of necessary WSSs and complicated fiber interconnection can be greatly reduced. Although wavelength collision could occur at intra-node fibers, it has been proven that the impact of this can be minimized by using a routing and wavelength assignment (RWA) algorithm that is aware of the intra-node restriction [4]. Our scheme [see Fig. 1(c)] seems to increase the number of WSSs to be traversed; the spectrum narrowing caused by traversing many WSSs strictly shortens the transmittable distance of signals. However, fewer WSSs are actually traversed than with the conventional OXC since the conventional OXC must employ the route-and-select architecture. This is because for the subsystem-modular OXC, the RWA algorithm can suppress the multiple traversals of sub-OXCs in a node with virtually no deterioration in fiber utilization [13]. Indeed, it has been confirmed that 90–80% of optical paths traverse only one sub-OXC in a node [13]. We can thus reduce the total number of

TABLE II
NETWORK TOPOLOGIES AND THEIR CHARACTERISTICS

Network topology				
Number of nodes		29	11	14
Node degree	Max.	7	8	5
	Min.	2	2	2
	Ave.	2.83	4.18	2.71
Number of links		41	23	19

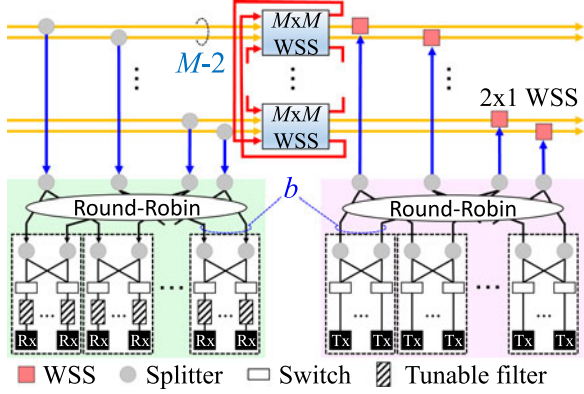


Fig. 2. The add/drop part employed transponder architecture.

traversed WSSs for each optical path from the source to destination and manage the impacts of noise and filtering depending on the required transmission characteristics. Obviously, applying an $M \times M$ WSS as a sub-OXC further simplifies the configuration as shown in Fig. 1(d). The OXC scale can be expanded simply by adding $M \times M$ WSSs.

Presently, 1×9 or 1×20 WSSs are commonly utilized. However, an $M \times M$ WSS is a more complicated device than the $1 \times M$ WSS, and past research-phase implementations reported so far have topped out at M of 5 or 8 [6]–[10] for $M \times M$ WSS. Thus, the port count, M , of the $M \times M$ WSS that will be commercialized in the near future is expected to be small. The subsystem-modular architecture can make the best use of such small-scale $M \times M$ WSSs [5]. To construct a 40×40 OXC, the conventional non-restricted OXC needs 160 1×20 WSSs and more than 1,600 interconnection fibers whereas the subsystem-modular OXC using 6×6 WSSs needs only 10 6×6 WSSs and just 20 interconnection fibers. An erbium-doped fiber amplifiers (EDFAs) are needed on each intra-node fiber connecting subsystem; omitted for simplicity in Fig. 1(c). The number of EDFAs needed in an OXC node is dominated by that in the add/drop part. Our add/drop architecture can reduce the number of EDFAs [5]. Different add/drop part architectures and the necessary number of EDFAs are discussed in detail in [5]. Thus, our architecture can be much more compact than the conventional architecture, and its effectiveness increases as the necessary OXC port-count increases.

Another point to be noted is the reliability of the OXC that uses $M \times M$ WSSs. The $M \times M$ WSS functions are integrated

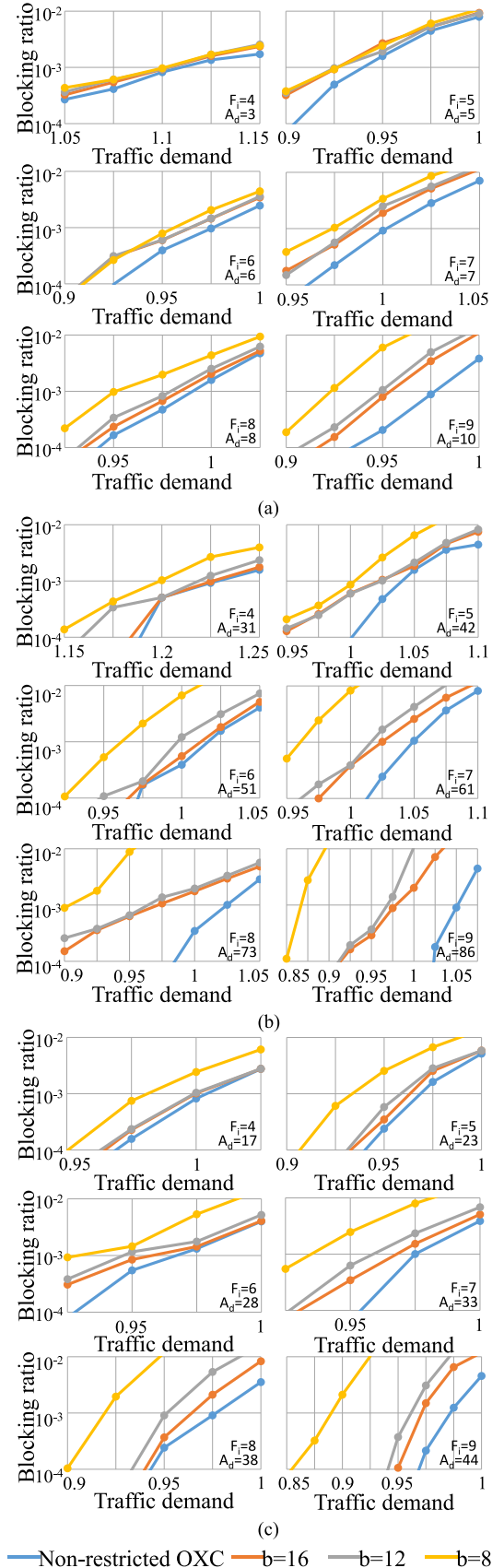


Fig. 3. Calculated blocking ratio, where F_i denotes the maximum number of sub-OXC stages and A_d represents the average path demand between nodes which is used to decide the arrangement of inter-node fibers.

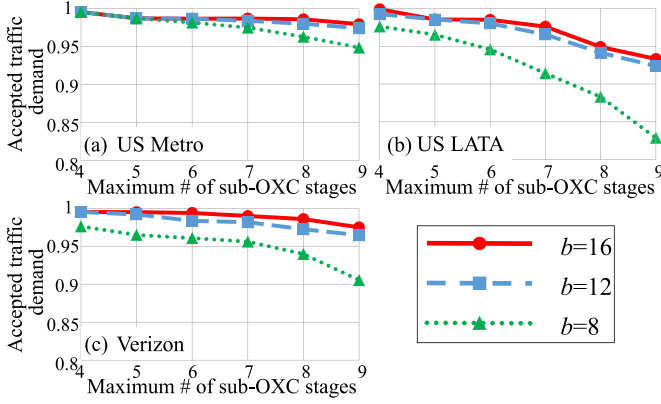


Fig. 4. Accepted traffic demand at blocking ratio of 10^{-3} .

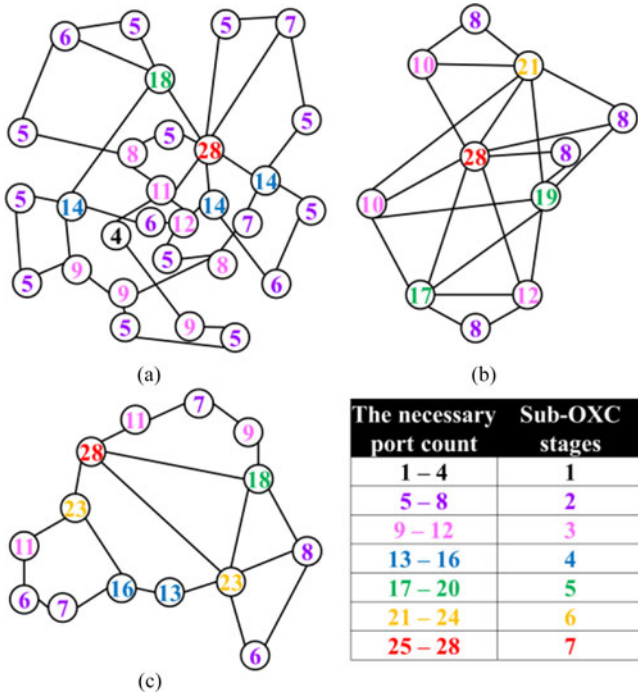


Fig. 5. The necessary port count for each node in (a) US Metro, (b) US LATA, and (c) Verizon networks when the maximum OXC port count is 28 in each network.

into the $M \times M$ WSS, and hence the failure rate may be higher than that of $1 \times M$ WSS, and the failure of an $M \times M$ WSS may impact more link fibers. These concerns are resolved by simply adding a protection $M \times M$ WSS module, if necessary, within the OXC, which assures the creation of highly reliable nodes and removes the single-point-of-failure concern at the same time [14], [15].

III. NETWORK SIMULATIONS

To evaluate the routing performance of the OXC using 6×6 WSS, we conduct computer simulations on metro networks under dynamic traffic scenarios. The network topologies tested are a version of US Metro [16], US LATA [17], and Verizon

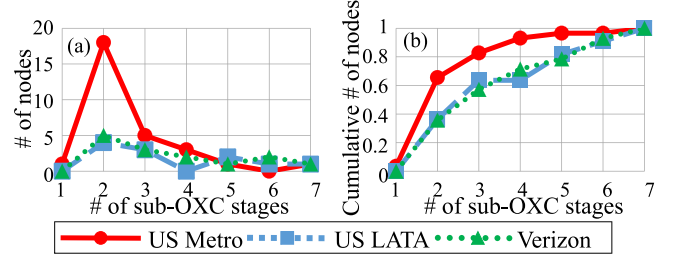


Fig. 6. (a) Distribution and (b) cumulative distribution, of the number of sub-OXC stages in a node.

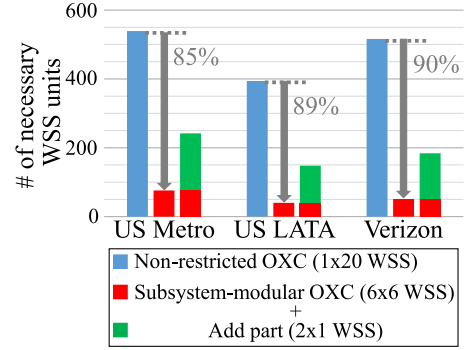


Fig. 7. The number of necessary WSS units in the whole network.

[18] metro networks, see Table II. To evaluate the differences among the physical topologies, we assumed that the traffic was uniformly and randomly distributed. The maximum number of wavelengths per fiber is 96. Within the OXC, the maximum number of intra-node fibers traversed by each path is limited to 4. The add/drop parts employ the transponder-bank structure shown in Fig. 2 [5]. This add/drop architecture has scalability equaling that of the OXC since transponders are divided into several groups and the number of fibers connected to each bank, b , is limited. In these simulations, parameter b is set at 8, 12 or 16. Here, routing flexibility and hardware requirements can be controlled via b ; smaller b reduces the number of EDFAs needed thanks to the decreased splitter loss, whereas larger b offers reduced blocking probability in add/drop parts since more banks connect to each add/drop fiber [5]. In the future large-traffic scenario, the splitter-EDFA combination is necessary to distribute a signal to many receivers [5]; the arrangement of splitters and EDFAs depends on the network parameters and hence the description of EDFAs is omitted for simplicity in Fig. 2. Our scheme properly bounds the number of accessible receivers to reduce the splitter degree as well as the number/gain of EDFAs, and the impact of the routing restriction is effectively resolved by using the restriction-aware routing algorithm. The add part is almost the same as the drop part; however, a combination of WSS and EDFA is needed to aggregate a large number of add signals. In Fig. 2, we depicted small-scale 2×1 WSS to remove amplifier noise in the add part; this 2×1 WSS can be removed if we employ the add/drop architecture shown in [5]. First, we conduct preliminary simulations on static networks assuming non-restricted OXCs under some expected traffic demand and

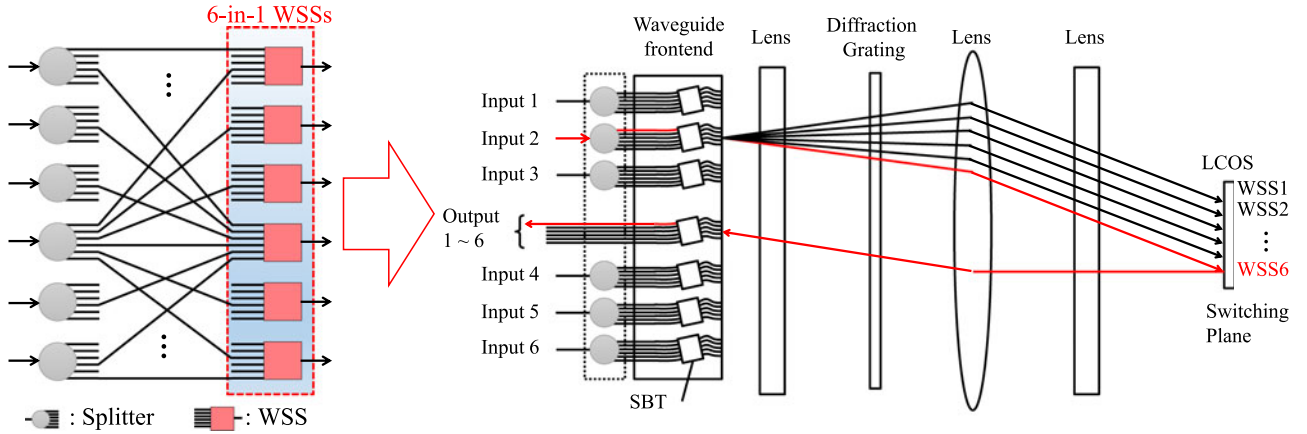
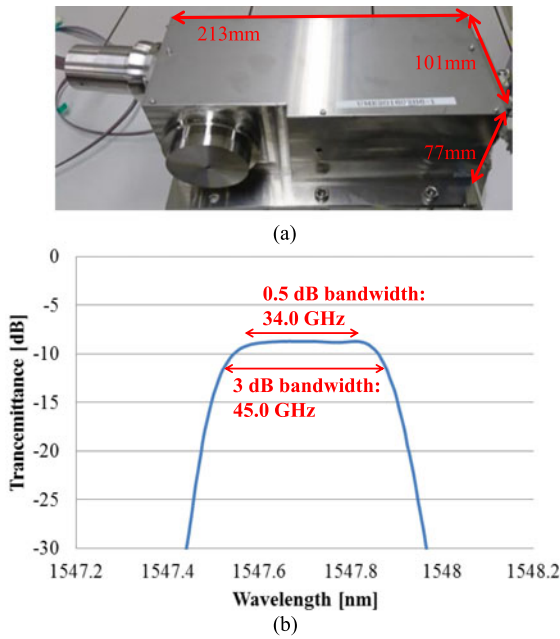
Fig. 8. Functional diagram and schematic diagram of 6×6 WSS.

Fig. 9. WSS prototype, (a) outlook and (b) an example of filtering function.

derive the necessary number of inter-node fibers. Using the derived networks, we evaluate routing performance under dynamic traffic scenarios. The average traffic demand between nodes is adjusted in each topology so that the maximum number of inter-node fibers in the network is changed from 16 to 36 which correspond to 4 to 9 sub-OXC stages, respectively.

Fig. 3 plots the blocking ratio obtained by simulations assuming dynamic traffic scenarios, as a function of the traffic demand normalized against the traffic demand indicated as A_d in Fig. 3, and the demand is used to decide the arrangement of inter-node fibers. As an example, we focus on the performance around the blocking ratio of 10^{-3} . From these evaluations, we derive the accepted traffic demand that is defined as the ratio of traffic demand accommodated with the proposed scheme to that with the ideal non-restricted OXC. Fig. 4 shows the normalized accepted traffic demand at the blocking ratio of 10^{-3} versus the maxi-

imum number of sub-OXC stages in each network. Compared to the ideal non-restricted OXC, the accepted traffic demand of the proposed scheme decreases as the maximum number of sub-OXC stages increases. This is because an increase in sub-OXC stages results in an increase in intra-node fibers, which enhances the chance of multiple intra-node fiber traversal and thus the possibility of intra-node blocking. Fig. 5(a), (b), (c) illustrate the necessary OXC port count for each node in the US Metro, US LATA, and Verizon networks, respectively. Here, the traffic demand is set so that the maximum OXC port count in each network is 28. We find that the necessary port count differs significantly among nodes in each network; this clearly shows that the importance of the pay-as-you-grow feature, which is gracefully realized with the subsystem-modular OXC. This feature is also critical given the continuous Internet traffic growth environment. Fig. 6(a) shows the distribution of the number of sub-OXC stages and Fig. 6(b) depicts its cumulative distribution function, where the maximum number of sub-OXC stages is 7. For all the networks tested, 80% of nodes need fewer than 5 stages and hence wavelength contention at intra-node fibers is well relaxed. Of particular interest, the US Metro topology attains the largest acceptable traffic (see Fig. 4) since it has more small-stage nodes and hence the blocking originating from intra-node fibers is smaller. Comparing US LATA and Verizon topologies, acceptable traffic for US LATA is more affected by OXC port count (maximum # of sub-OXC stages), as shown in Fig. 4. This is because US LATA (8) has much larger maximum node degree (cf. Table. II) than the number of inter-node fibers of each sub-OXC (4), probability of using intra-node fibers is much larger, which results in increased intra-node blocking [19]. In all cases, however, we can attain the desired OXC port count of 28 with less than 3% performance offset when $b = 16$.

Fig. 7 shows the total number of 6×6 WSSs necessary in each network at the traffic volume corresponding to the needed maximum OXC scale of 28, where the number of 2×1 WSSs needed for signal add is separately depicted. As a reference, the total number of 1×20 WSSs necessary for the non-restricted route-and-select OXC is also shown. Significant hardware reductions and system simplification can be attained; by using 6×6 WSSs, substantial cost reduction will be assured even if 6×6

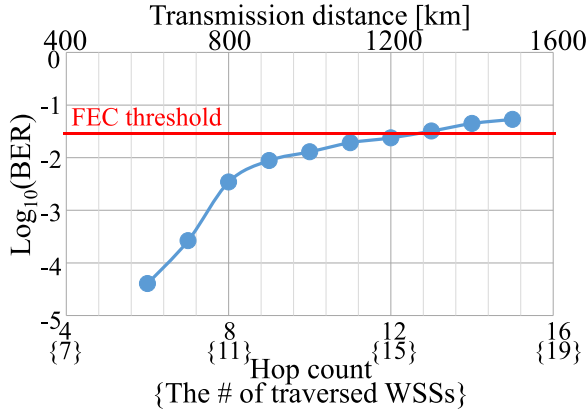


Fig. 11. BER measured as a function of hop count, where inter-node distance is 100 km.

#2 is off. Then, the two switch states were changed, and loop transmission started to send the signal from loop switch #2 to input #4. After multiple loops, the target signal traversed output #4, input #5, output #5, input #6, and output #6 in this order, where the non-target signals were updated at every output port. These operations correspond to traversing two intra-node fibers. The signals were then transmitted over a 100-km SMF and the target signal was finally detected by a digital coherent receiver. The signal was sampled by a 4-ch analog-to-digital converter (ADC) at 50 GSamples/s. After digital-signal processing, the bit-error ratio (BER) was calculated. Fig. 10(c) illustrates the relationship among time, switch states, and the number of loops that the signal experienced. With synchronized triggers, we can measure the transmission performance with the target loop count.

Fig. 11 shows BERs measured as a function of hop count; wavelength of 1547.316 nm was evaluated. Note that the number of traversed WSSs is given by hop count plus 3, which includes intra-node traversal. If we accept the limit BER of 2.7×10^{-2} assuming forward-error correction use, 12 node hops can be achieved; in this case, the number of 6×6 WSSs traversed is 16. The equivalent transmission distance is 1,200 km. This hop count and transmission distance cover most metro-network applications. We can expect further performance improvement by optimizing the 6×6 WSS characteristics.

VI. CONCLUSION

We demonstrated a subsystem-modular OXC that uses a newly developed 6×6 WSS. Based on extensive computer simulations, we verified its good network performance and cost-effectiveness. Indeed, the OXC inter-node fiber port count of 28 can be attained with a marginal ($<3\%$) routing-performance offset. The number of necessary 6×6 WSSs in the network was just 15–10% of that of the 1×20 WSSs needed with the conventional node architecture. The technical feasibility of the 6×6 WSS prototype was confirmed via transmission experiments. The hop count of 12 and transmission distance of 1,200 km were achieved with 96-wavelength 32-Gbaud signals. Further performance improvements in $M \times M$ WSSs are expected in the near future and will be reported elsewhere. Our

proposed OXC architecture is thus particularly suited to metro networks.

REFERENCES

- [1] “Cisco visual networking index: Forecast and methodology, pp. 2014–2019, May 27, 2015.
- [2] K. Sato, “Optical networking and node technologies for creating cost effective bandwidth abundant networks,” in *Proc. Opto Electron. Commun. Conf./Photon. Switching*, Niigata, Japan, 2016, Paper ThA1-2.
- [3] S. L. Woodward, M. D. Feuer, and P. Palacharla, “ROADM-node architectures for reconfigurable photonic networks” in *Optical Fiber Telecommunications*, I. P. Kaminow, T. Li, and A. E. Willner, 6th ed. Waltham, MA, USA: Academic, 2013, ch. 15, sec. 2, pp. 686–696.
- [4] Y. Tanaka *et al.*, “Criteria for selecting subsystem configuration in creating large-scale OXCs,” *J. Opt. Commun. Netw.*, vol. 7, no. 10, pp. 1009–1017, 2015.
- [5] M. Niwa *et al.*, “Tipping point for the future scalable OXC-What size $M \times M$ WSS is needed?,” *J. Opt. Commun. Netw.*, vol. 9, no. 1, pp. A18–A25, 2017.
- [6] K. Yamaguchi *et al.*, “ $M \times N$ wavelength selective switches using beam splitting by space light modulator,” in *Proc. Opto Electron. Commun. Conf.*, Shanghai, China, 2015, Paper PWe.08.
- [7] N. Nemoto *et al.*, “ 8×8 wavelength cross connect with add/drop ports integrated in spatial and planar optical circuit,” in *Proc. Eur. Conf. Opt. Commun.*, Valencia, Spain, 2015, Paper Tu.3.5.1.
- [8] N. K. Fontaine *et al.*, “ $N \times M$ wavelength selective crossconnect with flexible passbands,” in *Proc. Opt. Fiber Commun. Conf. Exhib.*, Los Angeles, CA, USA, 2012, Paper PDP5B.2.
- [9] L. Zong *et al.*, “Demonstration of ultra-compact contentionless-ROADM based on flexible wavelength router,” in *Proc. Eur. Conf. Opt. Commun.*, France, Italy, 2014, Paper P.4.4.
- [10] H. Uetsuka *et al.*, “ 5×5 wavelength cross-connect switch with densely integrated MEMS mirrors,” in *Proc. Photon. Switching*, San Diego, CA, USA, 2014, Paper PW2B.2.
- [11] K. Suzuki, K. Seno, and Y. Ikuma, “Application of waveguide/free-space optics hybrid to ROADM device,” *J. Lightw. Technol.*, vol. 35, no. 4, pp. 596–606, Feb. 2017.
- [12] R. Hashimoto *et al.*, “First demonstration of subsystem-modular optical cross-connect using single-module 6×6 WSS,” in *Proc. Eur. Conf. Opt. Commun.*, Gothenburg, Sweden, 2017, Paper Tu.2.F.2.
- [13] K. Sato *et al.*, “Disruption free expansion of protected optical path networks that utilize subsystem modular OXC nodes,” *J. Opt. Commun. Netw.*, vol. 8, no. 7, pp. 476–485, 2016.
- [14] S. Yamakami *et al.*, “Highly reliable large-scale optical cross-connect architecture utilizing $M \times M$ wavelength-selective switches,” in *Proc. Opt. Fiber Commun. Conf. Exhib.*, Los Angeles, CA, USA, 2017, Paper Th3K.5.
- [15] S. Yamakami *et al.*, “Highly reliable and large-scale subsystem-modular optical cross-connect,” *Opt. Express*, vol. 25, no. 15, pp. 17982–17994, Jul. 2017.
- [16] N. Madamopoulos *et al.*, “Metro network architecture scenarios, equipment requirements and implications for carriers,” in *Proc. Opt. Fiber Commun. Conf. Exhib.*, Anaheim, CA, USA, 2001, Paper WL2.
- [17] X. J. Zhang *et al.*, “Dimensioning WDM networks for dynamic routing of evolving traffic,” *J. Opt. Commun. Netw.*, vol. 2, no. 9, pp. 730–744, 2010.
- [18] G. Welbrock, “Metro 100G applications and technology,” in *Proc. Opt. Fiber Commun. Conf. Exhib./Nat. Fiber Opt. Eng. Conf.*, Anaheim, CA, USA, 2013.
- [19] K. Sato, “Impact of node/fiber/WSS degrees in creating cost effective OXCs,” in *Proc. 18th Int. Conf. Transp. Opt. Netw.*, Trento, Italy, 2016, Paper Th.B1.6.

Ryota Hashimoto received the B.E. degree from Nagoya University, Nagoya, Japan, in 2017, where he is currently working toward the M.E. degree at the Department of Information and Communication Engineering.

His research interest includes optical network, especially photonic network architecture and network design.

Shuhei Yamaoka received the B.E. degree from Nagoya University, Nagoya, Japan, in 2017, where he is currently working toward the M.E. degree at the Department of Information and Communication Engineering.

His research interest includes optical network, especially photonic network architecture and network design.

Yojiro Mori (M'15) received the Ph.D. degree in engineering from the University of Tokyo, Tokyo, Japan, in 2013. He is currently an Assistant Professor at Nagoya University, Nagoya, Japan. Before joining the university, he was a Research Fellow of the Japan Society for the Promotion of Science from 2011 to 2012. In 2013, he joined the Department of Electrical Engineering and Computer Science, Nagoya University. His current research interests include digital coherent technologies and optoelectronic devices for photonic networks.

Hiroshi Hasegawa (M'05) received the B.E., M.E., and D.E. degrees, all in electrical and electronic engineering, from Tokyo Institute of Technology, Tokyo, Japan, in 1995, 1997, and 2000, respectively.

He is currently an Associate Professor at Nagoya University, Nagoya, Japan. From 2000 to 2005, he was an Assistant Professor with the Department of Communications and Integrated Systems, Tokyo Institute of Technology. His current research interests include photonic networks, image processing (especially super-resolution), multidimensional digital signal processing, and time-frequency analysis.

Dr. Hasegawa is a member of the Institute of Electronics, Information and Communication Engineers (IEICE) and Society of Information Theory and its Applications (SITA). He was the recipient of the Young Researcher Awards from SITA and the IEICE in 2003 and 2005, respectively.

Ken-Ichi Sato (M'87–SM'95–F'99) received the B.S., M.S., and Ph.D. degrees in electronics engineering from the University of Tokyo, Tokyo, Japan, in 1976, 1978, and 1986, respectively.

He is currently a Professor with the Graduate School of Engineering, Nagoya University, Nagoya, Japan, and he is an NTT R&D Fellow. Before joining the university in April 2004, he was an Executive Manager of the Photonic Transport Network Laboratory, NTT. He has authored/co-authored more than 450 research publications in international journals and conferences. He holds 40 granted patents and more than 100 pending patents. He is a Fellow of the Institute of Electronics, Information and Communication Engineers (IEICE) of Japan. His most significant achievements lie in two of the important transport network technology developments. One is ATM (Asynchronous Transfer Mode) network technology, which includes the invention of the Virtual Path concept. The other is photonic network technology, which includes the invention of the optical path concept and various networking and system technologies. His contributions extend to coediting the *IEEE JOURNAL ON SELECTED AREAS IN COMMUNICATIONS* (four special issues) and the *JOURNAL OF LIGHTWAVE TECHNOLOGY* (three special issues); organizing several workshops and conference technical sessions; serving on numerous committees of international conferences including OFC 2016 General Chair and OFC 2014 Program Chair; authoring and coauthoring 14 books. He served as the President of the IEICE during 2016 and 2017. He was the recipient of the Young Engineer Award in 1984, the Excellent Paper Award in 1991, the Achievement Award in 2000, the Distinguished Achievement and Contributions Award in 2011 from the IEICE of Japan, and the Best Paper Awards in 2007 and 2008 from the IEICE Communications Society, the Distinguished Achievement Award of the Ministry of Education, Science and Culture in 2002, and the Medal of Honor with Purple Ribbon from Japan's Cabinet Office in 2014.

Keita Yamaguchi received the B.S. and M.S. degree in physics from Tsukuba University, Tsukuba, Japan, in 2009 and 2011. He joined Nippon Telegraph and Telephone (NTT) in 2011. He is currently with the NTT Device Technology Laboratories, Atsugi, Japan. He has recently been researching LCOS-based WSS and holographic phase modulation. He was the recipient of the Young Researcher's Award from the Institute of Electronics, Information and Communication Engineers (IEICE) of Japan in 2017. He is a member of the IEICE.

Kazunori Seno received the B.E. and M.E. degrees in material engineering from Tohoku University, Sendai, Japan, in 2004 and 2006, respectively. In 2006, he joined NTT Photonics Laboratories, Atsugi, Japan, where he was engaged in the research on optical devices based on spatial and planar optical circuit technology. From 2014 to 2016, he was engaged in the development of photonic transport network systems with NTT Network Service Systems Laboratories, Musashino, Japan. He is currently a Senior Research Engineer at NTT Device Technology Laboratories in Atsugi, Japan. He is a member of Institute of Electronics, Information and Communication Engineers of Japan.

Kenya Suzuki (M'00) received the B.E. and M.E. degrees in electrical engineering and the Dr. Eng. degree in electronics engineering from the University of Tokyo, Tokyo, Japan, in 1995, 1997, and 2000, respectively. He joined Nippon Telegraph and Telephone (NTT) in 2000. From September 2004 to September 2005, he was a Visiting Scientist with the Research Laboratory of Electronics, Massachusetts Institute of Technology. From 2008 to 2010, he was with the NTT Electronics Corporation, Ibaraki, Japan, where he was involved in the development and commercialization of silica-based waveguide devices. Since 2014, he has been a Guest Chair Professor at the Tokyo Institute of Technology, Meguro, Japan. He is currently at the NTT Device Technology Laboratories, Atsugi, Japan. His research interests include optical circuit design and optical signal processing. He was the recipient of the Young Engineer Award from the Institute of Electronics, Information and Communication Engineers (IEICE) of Japan in 2003. He is a Member of the IEICE, and the Physical Society of Japan.